

Protein Structure from Linear Dichroism Spectroscopy and Transient Electric Birefringence

Michael Bloemendal

Department of Protein and Molecular Biology, Royal Free Hospital School of Medicine, Rowland Hill Street, London NW3 2PF, U.K.

1 Perspective

Structural characterization of proteins plays an important role in fundamental science, medical research, and industry. X-Ray diffraction on protein crystals yields structures with a resolution better than 0.2 nm. However, many proteins, especially membrane-bound ones, resist crystallization. Moreover, the crystal structure may differ from the structure of the protein in its natural environment. Therefore, spectroscopic techniques to study biomolecules in solution are of great importance. Of these, nuclear magnetic resonance (NMR)* spectroscopy gives the most detailed results, but even for small molecules the spectra are complicated, and this problem becomes rapidly more severe with increasing size of the protein. Consequently, the applicability of NMR is restricted to smaller proteins (MW < 20 kDa).¹ In addition, both crystallographic X-ray diffraction and NMR experiments on proteins are time-consuming. Hence, these techniques are less appropriate for the comparison of a large set of mutants or closely related proteins, or for a single protein under different conditions. Moreover, the protein content in protein crystals is 50% or more and in NMR samples 1–10%, which is significantly higher than the physiological concentration for most proteins. Finally, these techniques have the disadvantage that relatively large quantities of proteins (5–10 mg at least) are required for accurate measurements.

In this paper, two less well-known techniques to study protein structures in solution, linear-dichroism (LD) spectroscopy and electric-field induced transient birefringence (ETB), will be discussed. From the former can be obtained information on the orientation of chromophoric groups in molecules, on molecular characteristics such as shape, size, and electronic properties, and on binding parameters in molecular complexes. From ETB hydrodynamic and electronic parameters, aggregational state, and intramolecular flexibility can be deduced. Both techniques are comparatively fast, and use relatively small quantities (0.2–2 mg) of protein at low concentration. After a general

Michael Bloemendal was born in Amsterdam, the Netherlands, in 1955. He obtained his B.Sc. in Chemistry, Biological Orientation (1977), and his M.Sc. (1980) and Ph.D. (1985) in Physical Chemistry (1985) at the Free University of Amsterdam. After postdoctoral research at the Hebrew University in Jerusalem, he was a recipient in 1987 of a C. & C. Huygens Fellowship from the Netherlands Organization for Scientific Research to study the influence of the medium on the structure of proteins with biophysical and analytical-chemical methods. Currently he is employed as senior research fellow at the Royal Free Hospital School of Medicine in London, where he is involved in the study of protein precipitation on biomedical materials.



description of the principles of the techniques, their application for the study of a specific lens-protein, α -crystallin, will be discussed in detail.

2 Linear-Dichroism Spectroscopy

2.1 The Concept

In optical spectroscopy, light interacts with parts of molecules, the so-called chromophores. The dominant interaction is that of the electric field of the light with the local charges on the chromophore. Effectively, light is absorbed when its frequency matches the difference in energy levels between two electronic states ($E = h\nu$), and – less generally realized – when the interaction yields an oscillating charge displacement on the chromophore.

This displacement is represented by the so-called transition dipole moment (TDM). Due to its oscillating character, it has an orientation but no direction! Different electronic transitions each induce a distinct TDM with characteristic orientation in a chromophore. Figure 1 shows those for UV absorption by indole, toluene, and phenol, the functional groups of tryptophan, phenylalanine, and tyrosine, respectively. As Figure 2 illustrates, charge displacement will be most effective, and hence absorption strongest, when the orientation of the electric field of the light coincides with that of the TDM. When the mutual angle

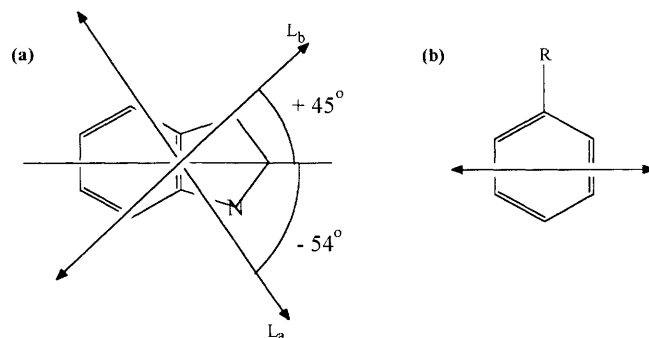


Figure 1 (a) The major transition dipole moments (\leftrightarrow), L_a and L_b , of indole according to Albinsson *et al.*;² (b) TDM of phenol (R = OH) or toluene (R = CH₃) according to Campbell and Dwek.³

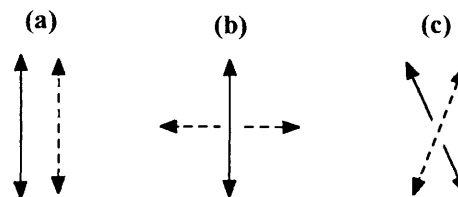


Figure 2 Interaction between the electric field of light ($\langle \dots \rangle$) and a transition dipole moment ($\langle \dots \rangle$): (a) maximum interaction; (b) no interaction; (c) intermediate interaction.

* ETB = electric field induced transient birefringence; FEA = fluorescence emission anisotropy; IF = intermediate filament; IgG = immunoglobulin-G; LD = linear dichroism; NMR = nuclear magnetic resonance; TDM = transition dipole moment

is 90°, no charge displacement and no absorption will take place. More generally, the absorption depends on both the size of the dipole moment, and the angle between the TDM and the electric field of the light. This means that when the orientation of the TDM is kept constant, the absorption of linearly polarized light by the chromophore depends on the direction of the polarization. The difference in absorption of two perpendicular polarized light beams, $\Delta_{LD}A$, is called the *linear dichroism* (LD). Hence,

$$\Delta_{LD}A = A_{\parallel} - A_{\perp} \quad (1)$$

Detailed reviews on LD-spectroscopy are given by Norden,⁴ Charney⁵ (electric-field induced LD), Norden *et al.*⁶ (especially LD on nucleic acids), and Bloemendal and van Grondelle⁷ (LD on proteins).

The simplest way to measure LD is by inserting a polarizer in front of the sample chamber of a conventional absorption spectrophotometer.^{2,7,8} However, most frequently a dedicated spectrophotometer is used that can generally be applied for both LD and circular-dichroism spectroscopy. Details have been described.^{4,6,7}

2.2 Orientation of the Sample

The necessity of constant orientation of the TDM implies that the molecules must have a net order within the time frame of the measurements. In most crystals and some biological systems, such as membranes, this is generally the case, but in a randomly oriented sample, as for example a protein in solution, special measures have to be taken in order to orient the molecules macroscopically. Orientation of biological molecules has been obtained in electric and magnetic fields, by electrophoretic orientation, in stretched polymer-films, liquid flow, liquid crystalline phases, natural and artificial membranes, lamellae and lipids, by shearing concentrated solutions on optical flats, by drying them in salt solution, by so-called wet-spinning, and in squeezed polyacrylamide gels (for details and references, see Bloemendal and Van Grondelle⁷). While the first three approaches orient the molecules according to their electric and/or magnetic properties, the others orient the particles with respect to their spacial symmetry axes. A special orientation mechanism, the so-called photoselection, is possible for photo-reactive compounds, where illumination with linearly polarized light leads to oriented photoproducts.⁸ The most commonly used orientation methods with some applications are collected in Table 1. It should be emphasized that none of the techniques mentioned produces fully ordered samples. Rather, a preferen-

tial direction of the molecules is obtained, where the extent of orientation depends on molecular properties like size and/or shape and, when electromagnetic fields are used, on dipole moments and polarizabilities or magnetic susceptibilities. Since the intensity of the LD depends on the degree of orientation, this can be used to extract information on these properties from the LD measurements.

Although in principle LD can be measured on almost any commercially available CD spectrophotometer, generally a special device has to be mounted into the spectrophotometer to produce and maintain a net order of the molecules.

2.3 Information from LD

2.3.1 General Consideration

As explained in Section 2.1, LD is caused by the dependence of the absorption of linearly polarized light by a chromophore on the angle between the TDM of that chromophore and the direction of polarization. This angle can be decomposed into the angle ξ of the TDM with a certain axis in the molecule, and the angle between that axis and the direction of polarization. The latter will depend on the mechanism and degree of orientation. Mathematically this means that $\Delta_{LD}A$ is a function (f) of ξ and an orientation factor ϕ ,

$$\Delta_{LD}A = f(\xi, \phi) \quad (2)$$

For several orientation techniques and differently shaped molecules, expressions for $f(\xi, \phi)$ have been derived.⁴⁻⁷ Different types of information obtained for biomolecules are given in Table 2, and will be discussed in the subsequent sections.

2.3.2 Orientation of Chromophores

Equation 2 implies that, when the orientations of the TDMs in the chromophore and those of the molecules in the sample are known, LD yields data on the orientation of the chromophores in the molecules. This is illustrated in Figure 3 for the tryptophans of bovine γ II-crystallin, a 21 kDa monomeric lens protein containing 4 Trp and 15 Tyr residues. As Figure 1 shows, Trp has two dominating TDMs (called L_a and L_b) for UV-absorption. The (sub)spectra belonging to these TDMs are different and slightly shifted.² By measuring LD as a function of wavelength information on the orientation of these two TDMs in γ -crystallin, and thus on the average position of the tryptophans with respect to the molecular axes, can be extracted.⁹ By using light of different wavelengths, information can be obtained on the orientation of various chromophores. An overview is given in Table 3.

Table 1 Some techniques for sample orientation in LD-spectroscopy and their biological applications^a

Technique	Some applications
Electric field	Chloroplasts, reaction centres, chlorophyll-protein interaction
Flow	Nucleic acids, nucleic acid-protein complexes
Stretched film	Nucleic acids
Squeezed polymer gel	DNA-protein interaction, coenzyme reorientation, proteins, pigment-complexes
Photoselection	Photoreactive compounds, retinal, bacteriorhodopsin
Shearing	Nucleic acids
Drying in salt solution	Nucleic acids, reaction centres, pigment-protein complexes
Wet-spinning	Nucleic acids
Electrophoresis	Proteins

^a For details and references see M. Bloemendal and R. van Grondelle *Mol Biol Rep* 1993 **18** 49.

Table 2 Some applications of LD-spectroscopy on biological molecules^a

Application	Example
Orientation of chromophores	γ Crystallin structure (see Section 2.3.2), Reorientation of chromophores during reaction
Global structure/electric parameters	γ -Crystallin structure (see Section 2.3.3)
Identification and quantification	Retinal isomers in complex mixtures (see Section 2.3.4)
Titration and binding	Protein binding to nucleic acids Ligand binding to macromolecules (see Section 2.3.5)

^a For details and references see M. Bloemendal and R. van Grondelle *Mol Biol Rep* 1993 **18** 49.

Gamma II Crystallin (bovine)

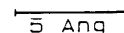
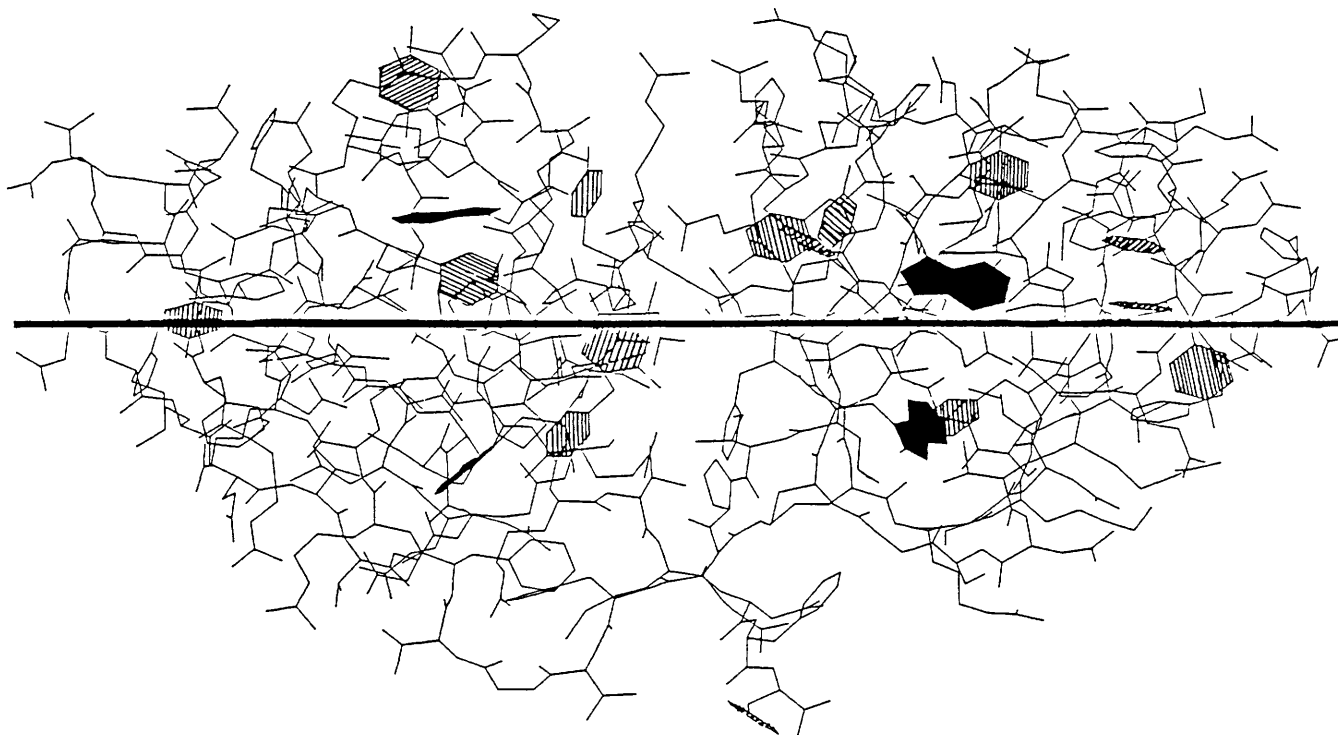

 5 Ang


Figure 3 The orientation of the tryptophans (black) and tyrosines (dashed) with respect to the long axis (black) of bovine γ II-crystallin (see Bloemendal *et al*⁹). Coordinates according to Wistow *et al*¹⁰ from Brookhaven Databank

Table 3 Chromophores used in LD spectroscopy of proteins and their band position^a

Chromophoric group	Band position
Aromatic residues	230–300 nm
Ligands/coenzymes/pigments	250–900 nm
Amide groups	3500–3000 cm^{-1} , 1700–1500 cm^{-1}
Carbonyls	1800–1600 cm^{-1}
Ethylene and aromatic proton bonds	1020–720 cm^{-1}
Nucleic acid interaction	240–350 nm

^a For examples and references, see M Bloemendal and R van Grondelle, *Mol Biol Rep* 1993 **18**, 49

2.3.3 Global Shape, Electric Properties

Alternatively, when the position of the TDMs in the chromophore and the conformation of the chromophores in the molecules are available, LD provides ϕ (see equation 2) and hence information on the parameters that govern the orientation of the sample (like shape, size, dipole moments, and so on). Figure 4 shows the absorption and LD spectra of bovine γ II- and γ IVa-crystallin. The X-ray structures of these closely related proteins have been determined at high resolution^{10–12}. The primary structures are 80% homologous, and the tertiary structures show only minor differences¹¹. The protein molecules were oriented in a one-dimensionally squeezed polyacrylamide gel according to van Amerongen *et al*^{13–15}. In this orientation technique the order of the molecules depends on their size (larger ones are better oriented) and shape (more spherical ones are less oriented)⁹. The absorption spectra look very similar, but the LD spectra are clearly different both in profile (the LD at 288 nm is positive for γ II and negative for γ IVa) and in magnitude. From a combination of the LD spectra and the X-ray structures the

orientation factors (ϕ in equation 2) for γ II and γ IVa were found to be 0.044 ± 0.006 and 0.018 ± 0.003 , respectively⁹. This means that γ II is much better oriented than γ IVa, which is a surprising result for two so-closely resembling proteins. A possible explanation is that, contrary to the situation in the crystal, the global shape of γ IVa in solution is more spherical than that of γ II. This interpretation is supported⁹ by size exclusion chromatography results,^{16,17} which yield a significantly smaller *apparent* molecular weight (and thus smaller excluded volume) for γ IVa-crystallin.

2.3.4 Identification and Quantification

The high sensitivity and specificity of the LD spectra of closely related compounds (see Figure 4) has been used to identify and quantify rare compounds in mixtures of closely related components¹⁸.

2.3.5 Binding and Titration

Unordered molecules do not yield LD ($\phi = 0$ in equation 2). This has been used in binding studies by means of LD with liquid flow orientation. Small molecules (even most proteins) are not oriented in a flow field. Therefore, the appearance of their absorption bands in the LD spectrum of a macromolecule like a nucleic acid is an extremely sensitive probe for their binding. This has been utilized for the calculation of equilibrium constants, the determination of binding sites, and the study of complex formation in titration studies (for references, see Nordén *et al*,⁶ and Bloemendal and van Grondelle⁷).

3 Electric Field Induced Transient Birefringence

3.1 The Concept

Particles with a permanent and/or inducible electric dipole moment can be oriented in solution by means of an electric field. For optically anisotropic particles this orientation leads to a difference in the refractive indices of the solution parallel (n_{\parallel}) and perpendicular (n_{\perp}) to the orientation direction,¹⁹ the so-called *birefringence*. When the electric field is switched on, the mole-

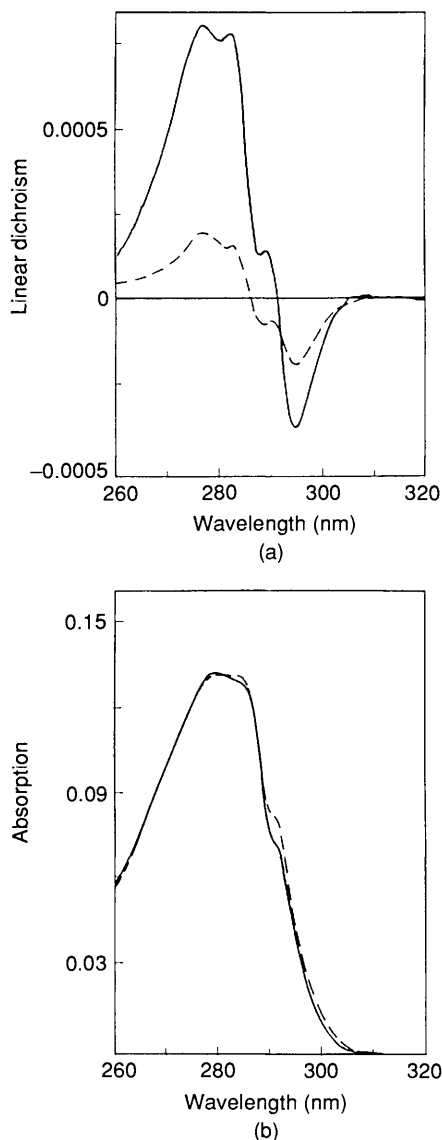


Figure 4 (a) LD and (b) absorption spectra of bovine γ II (—) and γ IVa (---) crystallin at identical concentration of protein (from Bloemendal *et al.*⁹).

cules become ordered and the birefringence ($\Delta n = n_{\parallel} - n_{\perp}$) is built up. When the field is switched off, the orientation and hence Δn decays due to the Brownian motion. This is illustrated in Figure 5 for a square pulsed electric field. The rate of orientation, and thus of the rise of Δn , depends on the hydrodynamic and electric properties of the particles, the steady state on the optical and electrical properties, and the (field-free) decay on hydrodynamic properties exclusively.

The primary quantity obtained from the decay is the rotational diffusion coefficient, which can be used to get information on molecular dimensions (shape and size), aggregational state and intramolecular flexibility.^{20–23} Molecular dimensions can, in principle, also be obtained from translational diffusion coefficients as reflected in centrifugation, viscosity, electrophoresis, and so on. However, rotational diffusion coefficients are much more sensitive and hence are a better probe for these properties.²⁴

Rotational diffusion coefficients can also be deduced from fluorescence emission anisotropy (FEA) measurements.²⁵ This technique is compared with ETB in Table 4. Although in principle FEA can be done on inherent fluorescent groups, like tyrosine or tryptophan residues, often an exogenous fluorescent group has to be attached to the molecules to be probed. ETB does not use external labels, and the time domain in which the

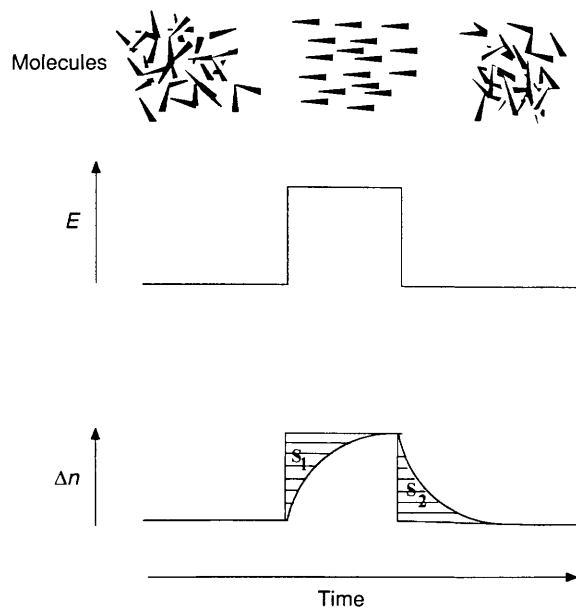


Figure 5 Electric field-induced transient birefringence: the molecules (dashes), the electric field (E), and the birefringence (Δn) as function of time. The dashed areas S_1 and S_2 are the areas enclosed by the rise and decay curves, respectively.

dynamics can be followed is not restricted by the life time of the fluorescent probe (usually < 100 ns). It enables the simultaneous study of rotational processes of molecular groups, monomers, and aggregates.^{20,23} Moreover, in ETB there are no restrictions to the pH range usable, whereas most fluorescent labels are non-fluorescent at low pH. Self-evidently, binding of a probe group always bears the risk of affecting the natural conformation of the molecules under study. A disadvantage of ETB is that relatively high fields are used to orient the molecules. This may influence the conformation or integrity of the molecules (this can be checked, see *e.g.* van Haeringen *et al.*^{20–22}), and restricts the range of ionic strengths that can be used for solutions in ETB. FEA has also the advantage that its response is restricted to the molecules (or molecular groups) where the fluorescent label is bound. Hence, this technique is more selective than ETB. Consequently ETB results are sometimes less straightforward to interpret.

Detailed reviews on (electric field induced transient) birefringence are given by Fredericq and Houssier¹⁹ and Charney.⁵ Recent literature on ETB is summarized by Stellwagen²⁶ and Curry and Krause.²⁷ Information on equipment can be found in these papers and that of van Haeringen *et al.*²⁰ Recently, an apparatus has been described, that may be used at physiological salt concentrations.²⁸

3.2 Information from ETB

3.2.1 Molecular Dimensions, Aggregation, and Flexibility

The decay of the birefringence after the electric field is switched off reflects the rotational relaxation of the particles that cause the birefringence (see Figure 5). Analysis of the decay as function of time yields rotational relaxation times (τ), which are related to the rotational diffusion coefficients. Asymmetric particles as well as multi-component samples yield multi-exponential decays. Computer programs like DISCRETE²⁹ and CONTIN³⁰ resolve the decays to provide the optimum number of relaxation times to describe the data. The use of these programs for ETB is discussed by van Haeringen *et al.*²⁰ Multiple relaxation is also found for particles that show internal flexibility. In that case some of the deduced relaxation times may reflect the orientation and disorientation of segments rather than molecules.¹⁹

Primarily, τ depends on the ratio between the viscosity (η) and

Table 4 Electric-field induced transient birefringence (ETB) versus fluorescence emission anisotropy (FEA) for determination of rotational diffusion coefficients^a

ETB	FEA
No external label	Fluorescent label (often exogenous)
Time domain upto microseconds	Time domain < 100 ns
No restriction on pH	Usually not possible at low pH
(High) electric field applied	No external field applied
Restricted ionic strength of solution	No restriction to ionic strength of solution

For discussion and explanation see text

the absolute temperature (*T*), and on the cube of the longest axis, *L*, of the rotating group

$$\tau \sim (\eta/T) L^3 \tag{3}$$

Expressions for the relation between τ and the dimensions of the molecules have been derived for differently shaped particles. Several of these are quoted in recent papers^{21–24, 26, 27}. When the relaxation is too fast to follow, the process can be retarded by increasing the viscosity of the solution, *e.g.* through addition of glycerol or sucrose, or by lowering the temperature. Equation 3 allows correction of the τ so-obtained to that at standard conditions.

In a study²⁰ of acid-induced structural changes of a mouse immunoglobulin G (IgG), several of the already-mentioned features of ETB are illustrated. IgG is a Y-shaped molecule as shown in Figure 6. Rotational relaxation times at two pH values in water and glycerol–water (40% w/v) are given in Table 5. In water at pH 6.6 a single relaxation is found, that corresponds to the rotation of the IgG monomer. The observed τ_2 of 151 ns agrees well with values obtained by other techniques³¹. After correction to the viscosity of pure water, the glycerol–water measurement yields the same rotation time (this is an essential test to see whether the viscosity change affects the global structure), but also indicates a fast relaxation process ($\tau_1 = 39$ ns). This time describes the segmental motion of the two IgG

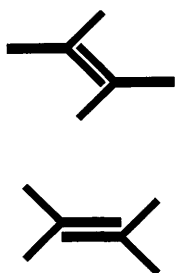


Figure 6 Two models for IgG dimerization at pH 2.7 based on ETB measurements from van Haeringen *et al.*²⁰. IgG monomers are represented by Y-shaped symbols

arms. At low pH this flexibility decreases (τ increases), and a third relaxation time is apparent. This slow time (440 ns) is due to aggregation at low pH. The ratio between τ_3 and τ_2 is about 3. Hence, equation 3 shows that the difference in length between the corresponding particles is $3^{1/3} = 1.4$. Also taking into account that the segmental flexibility is more or less retained, this result points to dimerization in one of the two forms given in Figure 6. The top arrangement would possibly involve considerable loss of segmental flexibility.

3.2.3 Electric Properties

The orientation of molecules in an electric field is caused by the torque exerted on their permanent and induced electric dipole moments. It has been shown that in the absence of a permanent dipole moment (μ_{perm}) the rate of birefringence build-up, due to the induced dipole moment (μ_{ind}) governed orientation, is equal to the rate of decay after switching off the electric field. The presence of a permanent dipole moment slows down the rise of the birefringence¹⁹. This can be used to estimate the relative contributions of μ_{perm} and μ_{ind} (called P/Q) to the orientation mechanism by taking the ratio between the areas excluded by the build-up curve and included by the decay curve, respectively (*S*₁ and *S*₂ in Figure 5). At low field strength where the birefringence is proportional to *E*², *S*₁/*S*₂ equals one for pure μ_{ind} caused orientation (P/Q = 0). For pure μ_{perm} ruled orientation (P/Q = ∞) it is four¹⁹. The assumption is that the orientation directions favoured by μ_{perm} and μ_{ind} are the same. Equations for the dependence of the orientation on the strength of μ_{perm} , μ_{ind} (reflected in the polarizability), and the electric field can be found in Fredericq and Houssier,¹⁹ and the references quoted there. Most biomacromolecules have an ionic atmosphere of counterions. These are polarized in an electric field. The induced dipole moment due to this ionic cloud is generally much stronger than the intrinsic μ_{ind} . In this case the induced dipole moment has a symmetry corresponding to the overall shape of the protein.

Kooijman *et al.*²³ have used *S*₁/*S*₂ calculations in their study of the building units of the intermediate filament (IF) protein, vimentin. The IF proteins are the major constituents of the cytoskeleton of most eukaryotic cells³². Although widely studied, there is no agreement on the size and structure of the primary units of these filaments^{23, 32}. Kooijman *et al.*²³ found a strong, although not exclusive, permanent dipole moment (*S*₁/*S*₂ = 3), which in combination with the observed multi-exponential decay indicated the presence of dimers, antiparallel tetramers, and hexamers (see Figure 7). The high value of *S*₁/*S*₂ is caused by the dipole moment of the dimers and hexamers.

3.2.4 Optical Anisotropy

The steady-state birefringence (Δn_0) is less straightforward to interpret, since its value is determined by both the optical and electric properties of the molecules. At low electric field, *E*, Δn_0 is proportional to the square of the external electric field strength ($\Delta n_0 = K_{kerr} E^2$), *K*_{kerr} being called the Kerr constant¹⁹. Kerr constants of IgG at different pH are included in Table 5. The value at pH 2.7 is clearly higher than that at 6.6. Moreover, there

Table 5 Rotational relaxation times (τ_i) and Kerr constants (*K*_{Kerr}) from ETB decays of IgG in water and water/glycerol (40% w/v) at two pHs^a

Solution	pH	τ_1 (ns)	τ_2 (ns)	τ_3 (ns)	<i>K</i> _{Kerr} (10 ⁻¹⁶ cm ² /V ²)
Water	6.6	–	151 ± 7	–	4.5 ± 0.1
Glycerol/water	6.6	39 ● 2	158 ± 1	–	NC
Water (after 1h)	2.7	NC	NC	NC	6.2 ± 0.2
Water (after 24h)	2.7	–	168 ± 11	411 ± 41	7.0 ± 0.2
Glycerol/water	2.7	51 ± 3	166 ± 8	438 ± 12	NC

^a Results from B. van Haeringen *et al.*²⁰ obtained by DISCRETE analysis of ETB decays. Indicated uncertainties are standard deviations of the mean values in glycerol/water are corrected to standard conditions (25°C viscosity of pure water). NC means not calculated.

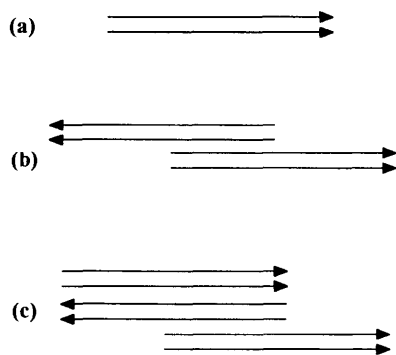


Figure 7 Building units of vimentin IFs indicated by S_1/S_2 calculation from ETB measurements:²³ (a) dimer with dipole moment; (b) antiparallel staggered tetramer without dipole moment; (c) hexamer with dipole moment. Each arrow represents a vimentin monomer with electric dipole moment.

is a further increase when the sample is kept at low pH for an extended period. Although separation of electric and optical effects is complicated, it is obvious that an instantaneous structural change followed by a slow process takes place. The latter might be the formation of aggregates as described in Section 3.2.1, whereas the fast process might be related to secondary structure changes that have been found immediately after decreasing the pH.³³

4 Application of LD and ETB to Study the Structure of α -Crystallin

4.1 Introduction

α -Crystallin, one of the predominant lens proteins, has attracted renewed interest since the detection of its occurrence in other tissues, and the discovery of its relation to heat-shock proteins.^{34,35} In lens α -crystallin contains 30–50 A- and B-type subunits (approximate ratio in bovine calf 3:1) with a molecular mass of 20 kDa/subunit and 60% sequence homology.³⁶ Despite extensive work by various groups, there is no consensus yet about its global shape and subunit-order. Some proposed a model in which the subunits are distributed in quasi-spherical or tetrahedral aggregates (see *e.g.* Tardieu *et al.*³⁷). Others also indicate more elongated structures.^{22,38} Pure α -crystallin is readily isolated by size-exclusion chromatography of dissolved lenses (see Figure 8)³⁹.

We have studied the structure of α -crystallin by ETB and LD.^{15,21,22} For LD measurements the protein molecules were oriented in one-dimensionally squeezed polymer gels, as described by Van Amerongen *et al.*^{13–15} The orientation mechanism in these gels is illustrated in Figure 9. In the undeformed meshwork, all orientations of the embedded molecules are equally probable. When the network is deformed, the molecules show an average preference for the long deformation axis of the gel. It is obvious from Figure 9 that spherical particles will not be oriented at all in the squeezed gel, and that a sample of tetrahedral particles will show no net orientation.

For orientation of a single chromophore in particles of rotational symmetry (disks, rods, ellipsoids) by this system, equation 2 becomes:^{7,13–15}

$$\frac{A_{LD}A}{A} = \phi \cdot \frac{3}{2} (3 \cos^2 \xi - 1) \quad (4)$$

where A is the isotropic (normal) absorption by the chromophore. For a system with more than one chromophore, equation 4 has to be summed over all chromophores:

$$\frac{A_{LD}A(\lambda)}{A(\lambda)} = \phi \cdot \frac{3}{2} \sum_{j=1}^N \left(\frac{A_j(\lambda)}{A(\lambda)} \langle 3 \cos^2 \xi_j - 1 \rangle \right) \quad (5)$$

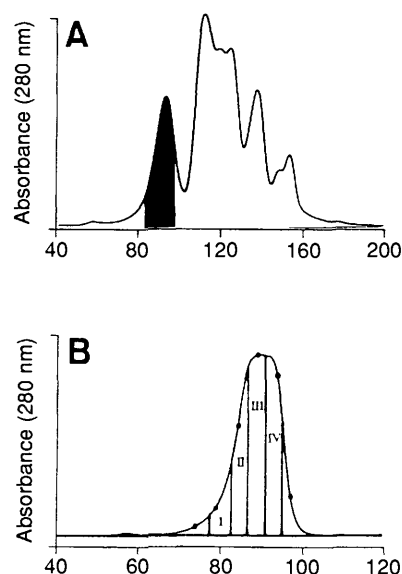


Figure 8 Isolation of α -crystallin: (a) Size-exclusion chromatography of dissolved lenses according to Vlaanderen *et al.*³⁹ The shaded area is used for analysis of total α -crystallin and for rechromatography. (b) Rechromatography of the shaded area of 8a to give subpools I–IV (from Van Haeringen *et al.*²²).

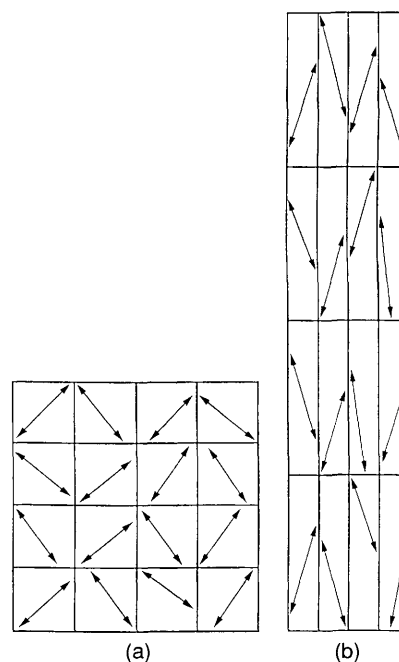


Figure 9 The orientation of particles represented by arrows in (a) an undeformed and (b) a deformed polymer meshwork.

where $A_j(\lambda)/A(\lambda)$ can be considered as the weight with which chromophore j contributes to the absorption at wavelength λ , and the brackets $\langle \dots \rangle$ denote the average over all chromophores of type j in the sample. ξ_j is the angle between the TDM and the symmetry axis of the particles. The orientation function ϕ has been given by Van Amerongen *et al.*¹³, and depends on the shape of the molecules and the degree of squeezing. For positive ϕ , $\xi = 54.7^\circ$ yields no LD; $\xi > 54.7^\circ$ gives negative LD; and $\xi < 54.7^\circ$ positive LD. In fact equations 4 and 5 hold for any particle with an axis (the orientation axis) around which the distribution is at least statistically rotationally symmetric.^{6,7}

4.2 Analysis of Total α -Crystallin Peak

4.2.1 Linear Dichroism

The LD and absorption spectra from 250 to 320 nm of bovine α -crystallin are shown in Figure 10. The fact that any LD spectrum is found, immediately refutes the idea that α -crystallin is spherically or tetrahedrally symmetric, since in that case no LD whatsoever would have been found (see Section 4.1). Apparently, at least part of the aggregates has a significant deviation from such symmetry. Between 250 and 350 nm, protein absorption spectra are essentially composed of the contributions of the aromatic residues tryptophan (Trp), tyrosine (Tyr), and phenylalanine (Phe). All these residues have their main TDMs in the plane of the aromatic ring. The absorption spectrum of Trp has maxima around 270, 280, and 290 nm, that of Tyr a single maximum at about 275 nm, and that of Phe a series of maxima between 250 and 265 nm. At its maximum the Trp absorption is about three and 25 times the maximal absorption for Tyr and Phe, respectively.⁴⁰ The occurrence of these residues in α -crystallin is 1, 6, and 14 per α A-, and 2, 2, and 13 per α B-subunit.³⁶ For an aggregate of 30 α A- and 10 α B-subunits this yields 50 Trp, 200 Tyr, and 650 Phe residues. One could expect such a number of chromophores in so many subunits to have all possible orientations. This would imply that absorption of parallel and perpendicular polarized light is almost equal. From equation 1 it appears that for such a case no LD is observed. Figure 10 shows not only that there is LD, but also that the LD spectrum resembles the absorption spectrum closely. Even the fine structure of the Phe absorption spectrum (250–265 nm, 650 residues in the aggregate) shows up in the LD spectrum. Apparently, there is a high structural order of the subunits within the aggregates and of the residues within the subunits, with a majority of the aromatic residues oriented in the same way. This contradicts models that assume a random orientation of the subunits in the α -crystallin aggregate. The fact that the LD is positive over the whole spectrum shows that the average angle ξ in equation 5 is smaller than 54.7°.

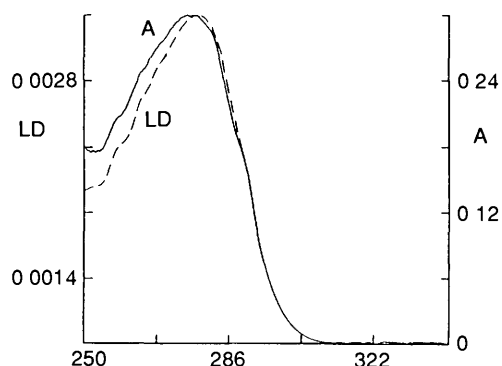


Figure 10 The absorption and LD spectra of bovine α -crystallin after orientation in a squeezed gel (from Bloemendal *et al.*¹⁵)

The magnitude of the LD varies from batch to batch. Values between 0.002 and 0.006 were found for the reduced dichroism, $A_{LD}A/(3AA)$, at 280 nm. This value is 2.5 to 7.5% of the theoretical value of a rigid rod-like protein with all the planes of the aromatic residues parallel to the long axis.¹⁵ For an aggregate of 30–50 subunits with about 900 aromatic residues this is a rather high value, again indicating a strong structural order of the subunits in the aggregates, and a significant deviation of spherical or tetrahedral symmetry for at least part of the molecules.

4.2.2 Electric Field-Induced Transient Birefringence

The decay of the ETB of α -crystallin appeared to be bi-exponential with relaxation times (τ) of 4 and 1 μ s, respectively.

Until a steady-state was reached the relative contribution of the slower time to the total decay of the birefringence increased, when longer electric pulses were used to orient the molecules.²¹ In general there are three possible explanations for a bi-exponential decay: (a) the rotation of a single type of molecules with asymmetric ellipsoid shape,²¹ (b) the rotation of a single type of molecules that contain internal flexibility (see Section 3.2.1), and (c) a mixture of two or more species. An asymmetric ellipsoid with $\tau_1/\tau_2 = 4$ would have a ratio of semi-axes of about 19.5:1 (see van Haeringen *et al.*²¹). Such an extreme elongation is completely in disagreement with all other evidence. Moreover, a single type of molecule is not likely to cause a change in relative contribution of the two times with duration of the electric pulse. Internal flexibility of the α -crystallin aggregate cannot be ruled out completely. However, electron microscopy pictures of α -crystallin give no indication whatsoever for a multi-lobal structure or extensions that could cause internal flexibility. Therefore the two times were interpreted as being caused by two different α -crystallin species. If both types were spherical, the ratio of relaxation times would directly reflect their volume ratio, since in that case τ corresponds to the cube of the radius (equation 3). Species with a volume ratio of four are separable by means of size-exclusion chromatography. No such separation has been reported yet. Moreover, the α -crystallin used for this study was taken from a single chromatographic peak (see Figure 8). Therefore it was concluded that α -crystallin as obtained from chromatography of dissolved lenses is composed of (at least) two differently shaped species. This conclusion is supported by the observed dependence on the pulse duration of the relative contribution of the relaxation times. Hydrodynamically smaller particles will orient faster. Hence, at pulse lengths that do not orient all the particles, their contribution to the signal will be relatively large. Increasing the pulse length will enhance the percentage of hydrodynamically larger particles that are oriented, and thus their contribution to the birefringence. Evidence for two differently shaped α -crystallins was also found from electron microscopy.²¹

4.3 Analysis of α -Crystallin Subpools

In order to study the structure of α -crystallin in more detail, the LD and ETB measurements were repeated on fractions of the total α -crystallin population. This was achieved by taking subpools of the original chromatographic peak, as illustrated in Figure 8. Average apparent molar masses determined from comparison with reference proteins are given in Table 6. Since separation on a gel filtration column is in fact not based on differences in mass, but on variation in Stokes' radius,⁴¹ the latter are also included in this table. Re-chromatography of the subpools did not lead to redistribution of molecular masses, which shows that the different α -crystallin species are not in reversible equilibrium with each other. Analysis of the ETB decay curves yielded two relaxation times for all pools, again indicating at least two different species for each pool. The faster of these times showed virtually no field strength and pulse duration dependence, suggesting that this time represents a well-defined particle. The slower relaxation time, on the contrary, showed variation with pulse strength and/or duration. Appar-

Table 6 Average apparent molecular masses (M_{app}) and Stokes' radii (R_S) of α -crystallin subpools determined from size exclusion chromatography^a

Pool	M_{app} (kDa)	R_S (nm)
I	1170 \pm 33	9.8 \pm 0.7
II	848 \pm 25	8.7 \pm 0.6
III	801 \pm 23	8.5 \pm 0.6
IV	745 \pm 22	8.3 \pm 0.6

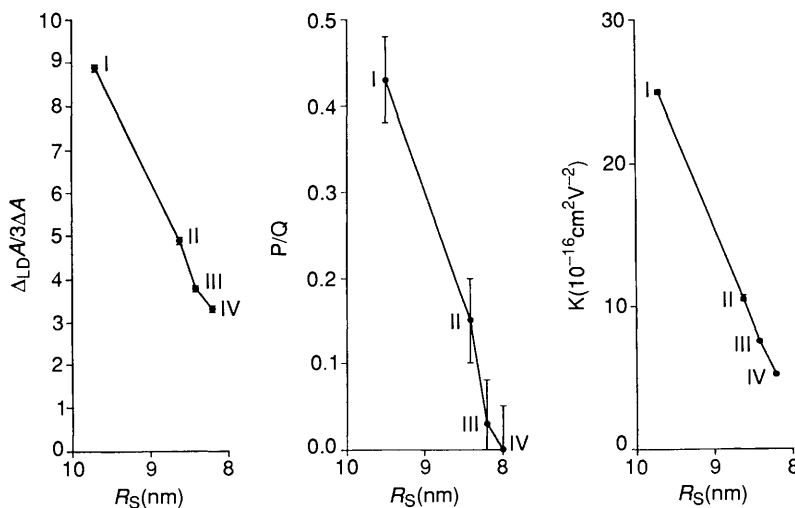
^a For discussion and explanation see text.

ently this time is related to a mixture of particles, and the subpools are still too large for complete homogeneity. For pool I the contribution of the slower time (about 6 μ s) to the total decay was 55%. For the other pools (5.0–5.5 μ s) it was only 20%. Combining these relaxation times with the Stokes' radii obtained from chromatography (Table 6) yields molecular dimensions, provided that a certain shape is assumed for the molecules.^{22,42} It appeared that the slow relaxation time can be related to cylindrically shaped particles with axial ratio between 3 and 6, and a diameter between 9 and 16 nm. In electron microscopy pictures of α -crystallin, asymmetric particles with axial ratios between 2 and 4 and diameters between 10 and 14 nm can be discerned among spherical ones.²¹ The fast time could be related with more or less spherical molecules (axial ratio \approx 1) and diameters of 13, 14, 15, and 23 nm for pools IV, III, II, and I, respectively (those of pool I show some deviation from sphericity).

Reduced LD at 280 nm, the ratio between the permanent and induced dipole contribution to the orientation (P/Q, see Section 3.2.3), and Kerr constants of the four pools as a function of their Stokes' radius are depicted in Figure 11. All quantities decrease from pool I to pool IV. The relatively high value of the LD of pool I can be explained by the larger contribution of asymmetric particles to this pool in comparison with the others (55% vs. 20%, see above). However, since no significant difference in the percentage of asymmetric particles is found for pools II, III, and IV, the further decrease cannot be explained in this way. Possibly the spherical α -crystallin molecules are not completely symmetric and are still oriented in the squeezed gel. In that case the size difference will cause the variation in LD. Alternatively there is a steady decrease in order of the subunits throughout the chromatographic peak of α -crystallin.

Interpretation of P/Q values and Kerr constants is less straightforward, since they are composed of contributions from both the slow and fast decaying particles. The P/Q value of pool IV is zero, which shows the absence of a permanent dipole moment for the particles of this pool. For pools III and II some permanent dipole contribution is found, whereas it is profound for pool I. Recalling that even pools II to IV contain 20% asymmetric particles, this shows that there is a decrease of permanent dipole moment throughout the chromatographic peak even within the asymmetric particles. This might be caused by a decrease in subunit order, which was also inferred from the decrease in LD. The observed Kerr constants also support this conclusion. The steady decrease from pool I to pool IV while the concentration of fast relaxing particles is similar for pools II to

Figure 11 Reduced linear dichroism ($\Delta_{LD}A/3\Delta A$) at 280nm, P/Q values, and Kerr constants *versus* the Stokes' radius as determined from size-exclusion chromatography for α -crystallin subpools denoted by Roman numerals.



IV points to different electric properties and/or optic anisotropy for both the symmetric and asymmetric particles.

4.4 Conclusion: A New Model for α -Crystallin

The combined results lead to the model for α -crystallin that is illustrated in Figure 12. α -Crystallin consists of two types of particles, a more or less symmetric one with a radius ranging from 13 to 23 nm, and an elongated one with axial ratio between 3 and 6 and diameter between 9 and 16 nm. The concentration of asymmetric particles is larger at the beginning of the chromatographic α -crystallin peak. There exists a significant order of the subunits within the molecules and of the aromatic residues within the subunits, the average angle between these residues and the long axis of the molecule being less than 54.7°. This order decreases throughout the chromatographic peak. Part of the molecules contain a strong permanent dipole moment. As this is especially found for the fraction that contains more elongated particles, these asymmetric structures may be particularly polar. However, even for the asymmetric molecules a decrease in polarity is found throughout the chromatographic peak.

Acknowledgement Dr. B. Van Haeringen is kindly acknowledged for his helpful remarks and critical reading of the manuscript, and the IRC for their financial support.

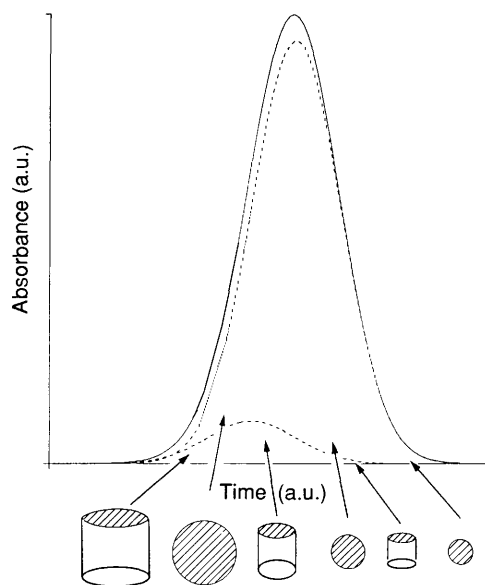


Figure 12 A model for α -crystallin.

5 References

- 1 G Wagner, S G Hyberts, and T F Havel, *Ann Rev Biophys Biomol Struct*, 1992, **21**, 167
- 2 B Albinsson, M Kubista, B Norden, and E W Thulstrup, *J Phys Chem*, 1989, **93**, 6646
- 3 I D Campbell and R A Dwek, 'Biological Spectroscopy', Benjamin/Cummings Publ, Menlo Park, CA, 1980, p 29
- 4 B Norden, *Appl Spectr Rev*, 1978, **14**, 157
- 5 E Charney, *Quart Rev Biophys*, 1988, **21**, 1
- 6 B Norden, M Kubista, and T Kurucsev, *Quart Rev Biophys*, 1992, **25**, 51
- 7 M Bloemendal and R van Grondelle, *Mol Biol Rep*, 1993, **18**, 49
- 8 K Fahmy, F Siebert, and P Tavan, *Biophys J*, 1991, **60**, 989
- 9 M Bloemendal, J A M Leunissen, H van Amerongen, and R van Grondelle, *J Mol Biol*, 1990, **216**, 181
- 10 G Wistow, B Turnell, L Summers, C Slingsby, D Moss, L Miller, P Lindley, and T Blundell, *J Mol Biol*, 1983, **170**, 175
- 11 H E White, H P C Driessen, C Slingsby, D S Moss, and P F Lindley, *J Mol Biol*, 1989, **207**, 217
- 12 T Blundell, P Lindley, L Miller, D Moss, C Slingsby, I Tickle, B Turnell, and G Wistow, *Nature*, 1981, **289**, 771
- 13 H van Amerongen, H Vasmel, and R van Grondelle, *Biophys J*, 1988, **54**, 65
- 14 H van Amerongen, M E Kuil, F van Mourik, and R van Grondelle, *J Mol Biol*, 1988, **204**, 397
- 15 M Bloemendal, H van Amerongen, H Bloemendal, and R van Grondelle, *Eur J Biochem*, 1989, **184**, 427
- 16 J G Bindels, J Bours, and H J Hoenders, *Mech Ageing Dev*, 1983, **21**, 1
- 17 R J Siezen, E Wu, E D Kaplan, J A Thomson, and G B Benedek, *J Mol Biol*, 1988, **199**, 475
- 18 J Horwitz and J Heller, *J Biol Chem*, 1973, **248**, 1051
- 19 E Fredericq and C Houssier, 'Electric Dichroism and Electric Birefringence', Clarendon Press, Oxford, 1973
- 20 B van Haeringen, W Jiskoot, R van Grondelle, and M Bloemendal, *J Biomol Struct Dyn*, 1992, **9**, 991
- 21 B van Haeringen, D Eden, M R van den Bogaerde, R van Grondelle, and M Bloemendal, *Eur J Biochem*, 1992, **210**, 211
- 22 B van Haeringen, M R van den Bogaerde, D Eden, R van Grondelle, and M Bloemendal, *Eur J Biochem*, 1993, **217**, 143
- 23 M Kooijman, M Bloemendal, H van Amerongen, P Traub, and R van Grondelle, *J Mol Biol*, 1994, **236**, 1241
- 24 J G Garcia de La Torre and V A Bloomfield, *Quart Rev Biophys*, 1981, **14**, 81
- 25 S B Brown, 'An Introduction to Spectroscopy for Biochemists', Academic Press, London, 1980, chapter 3
- 26 N C Stellwagen, *Biopolymers*, 1991, **31**, 1651
- 27 J F Curry and S Krause, *J Phys Chem*, 1992, **96**, 4643
- 28 D Porschke and A Obst, *Rev Sci Instrum*, 1991, **62**, 818
- 29 S W Provencher, *Biophys J*, 1976, **16**, 27
- 30 S W Provencher, *Comp Phys Commun*, 1982, **27**, 229
- 31 J Yguerabide, H F Epstein, and L Stryer, *J Mol Biol*, 1970, **51**, 573
- 32 P M Steinert and D R Roop, *Ann Rev Biochem*, 1988, **57**, 593
- 33 W Jiskoot, M Bloemendal, B van Haeringen, R van Grondelle E C Beuvery, J N Herron, and D J A Crommelin, *Eur J Biochem*, 1991, **201**, 223
- 34 D Jones, R H Russnak, R J Kay, and E P M Candido, *J Biol Chem*, 1986, **261**, 12006
- 35 S P Bhat, J Horwitz, A Srinivasan, and L Ding, *Eur J Biochem*, 1991, **102**, 775
- 36 H Bloemendal, *CRC Crit Rev Biochem*, 1982, **12**, 1
- 37 A Tardieu, D Laporte, P Licinio, B Krop, and M Delaye, *J Mol Biol*, 1986, **192**, 711
- 38 R C Augusteyn, E M Parkhill, and A Stevens, *Exp Eye Res*, 1992, **54**, 219
- 39 I Vlaanderen, R van Grondelle, and M Bloemendal, *J Liq Chromatogr*, 1993, **16**, 367
- 40 'Handbook of Biochemistry and Molecular Biology, Proteins', ed G Fasman, 3rd Edn, CRC Press Cleveland, 1976, Vol 1, pp 185—195
- 41 L C Davis, *J Chromatogr Sci*, 1983, **21**, 214
- 42 C Sadron, *Progr Biophys Biophys Chem*, 1953, **3**, 237